



GC-MS Profiling and Molecular Docking of Pistachio Shell (*Pistacia vera*): Insights into its Anticancer Potential Against Cervical Cancer Targets

Sugantha Swarna Manjari¹, Raju Balaji^{2*}

¹Saveetha Medical College and Hospital, Saveetha Institute of Medical and Technical Sciences (SIMATS), Saveetha University, Chennai 602105, Tamil Nadu, India

²Molecular Biology and Genomics Lab, Department of Orthopaedics, Saveetha Medical College and Hospital, Saveetha Institute of Medical and Technical Sciences (SIMATS), Saveetha University, Chennai 602105, Tamil Nadu, India

(Received: 16 February 2026

Revised: 25 March 2026

Accepted: 10 April 2026)

KEYWORDS

1,2-Cyclopentanedione,
Catechol,
Cervical cancer,
GC-MS,
Molecular docking,
Pistacia vera shell

ABSTRACT:

Background: Cervical cancer is one of the leading causes of cancer-related morbidity and mortality among women worldwide, particularly in low- and middle-income countries. The limitations of current therapies indicate that there is an urgent need for affordable, plant-derived alternatives. *Pistacia vera* (pistachio), a widely consumed nut crop valued for its nutritional and economic importance, generates shells as an agro-industrial byproduct. Rich in phenolics, fatty acids, sterols, and terpenoids, pistachio shells remain underexplored for their anticancer potential.

Objectives: The present study undertakes the first systematic evaluation of pistachio shell methanolic extracts against cervical cancer molecular targets. GC-MS profiling was employed to catalog the phytoconstituents, followed by molecular docking against HPV E6 (PDB: 4XR8) and tumor suppressor p53 (PDB: 1TUP).

Methods: Methanolic extracts of pistachio shells were subjected to GC-MS profiling to identify phytoconstituents. The detected metabolites were docked against cervical cancer-relevant targets, HPV E6 oncoprotein (4XR8) and tumor suppressor p53 (1TUP). ADMET and drug-likeness analyses were performed to evaluate pharmacokinetic feasibility and safety.

Results: GC-MS analysis revealed 32 bioactive constituents, including catechol, oleic acid, stigmaterol, betulin, and nimbin. Among them, 1,2-cyclopentanedione exhibited the strongest interaction with HPV E6 (−9.34 kcal/mol), while catechol showed the highest affinity for p53 (−9.45 kcal/mol). Other metabolites such as nimbin, d-mannose, and oleic acid demonstrated multi-target binding potential. ADMET predictions indicated favorable pharmacokinetic properties, with high gastrointestinal absorption, no CYP450 inhibition, and non-toxic profiles for most candidates, supporting their suitability for oral formulations.

Conclusions: This study provides the first integrated GC-MS and in silico evaluation of pistachio shell, identifying 1,2-cyclopentanedione and catechol as promising dual modulators of HPV E6 and p53. These findings emphasize the intriguing possibility of valuing pistachio agro-waste as a plant-based therapeutic against cervical cancer, warranting further preclinical and clinical investigations

1. Introduction

Cervical cancer remains a pressing global health challenge, ranking as the fourth most common cancer among women worldwide and a leading cause of mortality in low- and middle-income countries (LMICs). Globally, nearly 600,000 new cases are reported annually, with more than 300,000 deaths, the majority occurring in South Asia and Sub-Saharan Africa where access to human papillomavirus (HPV) vaccination, early detection, and advanced therapeutic facilities

remains limited [1]. In India alone, cervical cancer is projected to affect over 85,000 women annually by 2025, making it the second most common malignancy in women, with recent meta-analyses reporting HPV prevalence as high as 85% among cervical cancer patients [2]. The incidence of cervical cancer in India is strongly influenced by lack of screening and early detection, especially in rural communities where Pap smear-based studies have revealed a notable prevalence of premalignant lesions [3]. The etiology of cervical



cancer is tightly linked to persistent infection with high-risk HPV types, particularly HPV-16 and HPV-18, consistent with evidence that HPV infection is detected in the vast majority of cervical cancer cases in India [2]. Viral oncoproteins E6 and E7 drive oncogenesis by inactivating the tumor suppressors p53 and retinoblastoma (Rb), promoting genomic instability and malignant transformation [4]. Although chemotherapeutics such as cisplatin, paclitaxel, and topotecan constitute the standard of care, their utility is constrained by systemic toxicity, drug resistance, and lack of target specificity [5]. Therefore, the exploration of novel, safe, and affordable plant-derived compounds that can interfere with HPV-driven oncogenic pathways represents an urgent biomedical priority. Natural products, particularly phytochemicals from medicinal plants, have historically contributed to anticancer drug discovery. Compounds such as paclitaxel and vincristine exemplify the translational potential of phytochemicals. Recent advances in metabolomics, computational docking, and ADMET prediction now enable a systematic evaluation of underutilized plant resources for drug development. Agro-industrial byproducts, often considered waste, are increasingly being recognized as reservoirs of bioactive molecules with therapeutic applications. This “waste-to-wealth” paradigm offers a sustainable strategy for drug discovery while reducing environmental burden [6].

Pistacia vera L. (family Anacardiaceae), commonly known as Pistachio, is a nut crop cultivated extensively in Iran, Turkey, the USA, and Mediterranean countries. Pistachios are globally valued for their nutritional profile, being rich in proteins, unsaturated fatty acids, fibers, minerals, and antioxidants [7]. Beyond their dietary role, pistachios have long been utilized in traditional Persian, Chinese, and Mediterranean medicine for treating gastrointestinal disorders, hemorrhage, skin ailments, and respiratory complaints [8]. Modern phytochemical investigations have revealed a wide diversity of bioactives in pistachio kernels, pericarps, hulls, and shells, including phenolic acids, flavonoids, tannins, sterols, terpenoids, and anacardic acids [6,9]. These molecules exhibit strong antioxidant, anti-inflammatory, antimicrobial, cardioprotective, and anticancer activities. Among pistachio byproducts, the shells represent nearly 70% of the total biomass generated during dehulling and are currently

underutilized, typically burned for energy or discarded as waste [6,13]. Chemical profiling has shown that pistachio shells contain substantial amounts of lignin, cellulose, and bioactive polyphenols, making them attractive candidates for valorization in nutraceutical and pharmaceutical industries. Extracts of pistachio shells have demonstrated high antioxidant activity, α -glucosidase and α -amylase inhibitory potential, and cytotoxicity against various cancer cell lines [6]. Furthermore, shell-derived biofiller materials have been successfully incorporated into biodegradable films and polymer composites for food packaging, highlighting their sustainable applications [14].

Pharmacological research into *P. vera* has provided increasing evidence of anticancer activity. Falahati-Pour et al., [15] demonstrated that pistachio pericarp and kernel extracts synergistically enhanced the cytotoxic effects of cisplatin in prostate cancer PC-3 cells by upregulating pro-apoptotic genes (BAX, p53) and downregulating anti-apoptotic mediators (BCL-2, NANOG). Similarly, in another reported that ethanolic extracts of pistachio exhibited both antibacterial and anticancer activity, reducing viability in MCF-7 (breast) and A2780 (ovarian) cancer cell lines [8]. Further confirmed that pistachio hull fractions rich in gallic acid and quercetin induced apoptosis in breast cancer cells through caspase activation, Bax upregulation, and Bcl-2 suppression, and also inhibited tumor growth *in vivo* [9]. Collectively, these findings suggest that pistachio-derived phytochemicals exert anticancer effects via modulation of apoptosis, oxidative stress, and cell-cycle regulation. From a chemical perspective, pistachio hulls and shells are rich in polyphenols, including gallic acid, catechin, quercetin, cyanidin, luteolin, and anacardic acids, as well as fatty acids (oleic, linoleic, palmitic acids), phytosterols (stigmasterol, β -sitosterol), and triterpenoids (betulin) [10-12]. Many of these compounds are known for their anticancer potential. For instance, catechol and quercetin scavenge reactive oxygen species and trigger mitochondrial apoptosis; sterols like stigmasterol interfere with membrane signaling and proliferation; and betulin has been shown to suppress tumor angiogenesis. These bioactives may act individually or synergistically to suppress tumor progression. The valorization of pistachio shells aligns with current trends in sustainable bioprospecting. Large-scale pistachio production generates thousands of tons of



lignified shells annually, posing an environmental challenge. Transforming these residues into sources of therapeutic phytochemicals reduces waste and supports circular bioeconomy models [14]. Beyond biomedical applications, pistachio shells have also been investigated as bio-fillers in synthetic fiber/epoxy composites, highlighting their versatile utility as sustainable materials [16]. In particular, targeting cervical cancer through pistachio shell extracts represents a novel avenue, as no prior systematic study has explored their direct effects on HPV-related oncogenesis. Given the critical role of HPV E6 in p53 degradation, restoring p53 function while simultaneously inhibiting E6 represents a rational therapeutic strategy [17]. Computational approaches such as GC-MS-based metabolite identification, molecular docking, and ADMET modeling provide powerful tools to screen natural metabolites for such dual-target effects. Previous in silico studies on plant extracts have successfully predicted phytochemicals capable of binding HPV oncoproteins with high affinity, supporting the integration of computational pharmacology into natural product discovery.

2. Objectives

The present study undertakes the first systematic evaluation of pistachio shell methanolic extracts against cervical cancer molecular targets. GC-MS profiling was employed to catalog the phytoconstituents, followed by molecular docking against HPV E6 (PDB: 4XR8) and tumor suppressor p53 (PDB: 1TUP). Lead candidates such as catechol and 1,2-cyclopentanedione were identified with strong dual-target binding potential. Subsequent ADMET and drug-likeness predictions were conducted to assess pharmacokinetic suitability and toxicity. This integrative approach not only highlights pistachio shells as a novel waste-to-wealth phytochemical reservoir but also establishes a framework for developing cost-effective, plant-based therapeutics against cervical cancer.

3. Materials and Methods

Sample Collection and Preparation of Extract

Pistachio shells (*Pistacia vera* L.), a lignocellulosic agro-industrial byproduct obtained after kernel processing, were collected from a local dry fruit processing unit in Chennai, Tamil Nadu, India (GPS Coordinates: 13°04'35.0"N, 80°16'33.0"E) (Figure 1). The plant

material was taxonomically authenticated by Dr. K. Devanathan, Botanist, Department of Botany, The American College, Madurai-625002, Tamil Nadu, India. The collected shells were thoroughly washed with distilled water to remove adhering residues, shade-dried at ambient temperature (28 ± 2 °C) for 7 days, and ground into a fine powder using a mechanical grinder. For extraction, 10 g of powdered shell material was soaked in 100 mL of analytical-grade methanol (1:10 w/v) in a sterile conical flask. The flask was sealed and maintained in a rotary shaker at 37 °C for 48 h to facilitate cold maceration. The extract was filtered through Whatman No. 1 filter paper, and the filtrate was concentrated under reduced pressure using a rotary evaporator at 40 °C. The resulting crude methanolic extract was transferred to amber-colored vials and stored at 4 °C until subjected to GC-MS profiling and subsequent in silico analyses, including molecular docking, ADMET, and drug-likeness predictions.

Gas Chromatography-Mass Spectrometry (GC-MS) Analysis

The phytochemical constituents of the methanol extract of pistachio shells were analyzed using GC-MS. The analysis was performed on an Agilent GC 7890A system equipped with a 5975C inert XL EI/CI MSD mass selective detector. The chromatographic separation was achieved using a DB-5MS capillary column (30 m × 0.25 mm ID × 0.25 μm film thickness). The injection volume was 1 μL, administered in splitless mode. The oven temperature was initially set at 30°C, then ramped at 10°C/min to 350°C and held for 4 minutes. Helium (99.99%) was used as the carrier gas at a constant flow rate of 1 mL/min. The injector and transfer line temperatures were maintained at 280°C. Electron ionization was conducted at 70 eV, with the mass scan range set between 45 and 380 m/z. The acquired mass spectra were analyzed using the NIST 20 Mass Spectral Library to identify the components based on similarity index scores. Compounds were characterized by their retention time (RT), name, molecular formula, CAS number, match score, and relative abundance. The percentage composition of each compound was calculated based on peak area normalization.

Molecular docking against cervical cancer targets

Molecular docking studies were carried out to assess the binding affinity of bioactive phytochemicals identified



from the methanol extract of pistachio shells against cervical cancer-associated protein targets. The docking workflow was conducted using Schrödinger Suite 2021 (Schrödinger LLC, New York, USA). The chemical structures of the selected phytochemicals, identified through GC–MS profiling, were retrieved from the PubChem database (<https://pubchem.ncbi.nlm.nih.gov/>). Ligand structures were prepared using the LigPrep module, which generated three-dimensional conformations with accurate stereochemistry, ionization states (within the pH range 2.0 to 7.0), and up to 32 stereoisomers per ligand. Geometry optimization and energy minimization were performed using the OPLS_2005 force field. Two protein targets involved in cervical cancer pathways were selected based on their therapeutic relevance: Human Papillomavirus (HPV) E6 Protein – PDB ID: 4XR8 and p53 Tumor Suppressor Protein – PDB ID: 1TUP for cervical cancer. The 3D crystal structures of all protein targets were downloaded from the RCSB Protein Data Bank (<https://www.rcsb.org/>). Protein preparation was carried out using the Protein Preparation Wizard of the Schrödinger Suite, which included the assignment of bond orders, addition of hydrogen atoms, optimization of the hydrogen bonding network, correction of metal ion geometries, and removal of water molecules using the Epik module. Protonation states were assigned at physiological pH, and the protein structures were subjected to restrained energy minimization using the OPLS_2005 force field to ensure structural stability before molecular docking. Receptor grids were generated at the active sites of each protein using default van der Waals scaling factors and partial charge cut-off parameters. Molecular docking was conducted using the Glide module. Preliminary screening was performed in High Throughput Virtual Screening (HTVS) mode to filter potential binders. The top-ranking ligands were further refined using the Extra Precision (XP) mode. Binding affinities were assessed based on Glide G-scores, and the most favorable poses were selected for subsequent visualization and molecular interaction analysis.

Molecular Dynamics Simulation

The top-ranked protein–ligand complexes obtained from molecular docking were further subjected to Molecular Dynamics (MD) simulations using Desmond v3, integrated within the Schrödinger Suite. Each complex

was embedded in an orthorhombic simulation box and solvated using the Single Point Charge (SPC) water model. System neutrality was achieved by adding appropriate numbers of Na⁺ and Cl[−] counterions. Prior to simulation, energy minimization was performed to relax the system and remove steric clashes. MD simulations were then conducted for a duration of 100 nanoseconds under NPT ensemble conditions, with a constant temperature of 300 K and pressure of 1.013 bar. Temperature and pressure were maintained using the Nosé–Hoover chain thermostat and Martyna–Tobias–Klein barostat, respectively. The OPLS_2005 force field was applied throughout the simulation for both protein and ligand. Post-simulation trajectory analyses were carried out to assess the structural stability and flexibility of the protein–ligand complexes. Key parameters such as Root Mean Square Deviation (RMSD) and Root Mean Square Fluctuation (RMSF) were computed to evaluate the conformational dynamics and binding stability of the ligands within the active sites of the target proteins.

Principal Component Analysis (PCA) and Free Energy Landscape (FEL)

Principal Component Analysis (PCA) was conducted to further explore the conformational space and dominant motion patterns of the protein–ligand complexes during molecular dynamics simulations. PCA was performed on the C α atoms of the protein backbone to extract the essential dynamics by reducing the dimensionality of atomic motions. The covariance matrix of atomic positional fluctuations was calculated and diagonalized to obtain eigenvalues and eigenvectors, which represent the amplitude and direction of motion, respectively. The first two principal components (PC1 and PC2) were used to construct a two-dimensional projection plot, thereby visualizing the dominant conformational transitions. Subsequently, a Free Energy Landscape (FEL) analysis was performed using the same PC1 and PC2 data to map the thermodynamically stable states of the protein–ligand complexes. The free energy was calculated based on the probability distribution of conformations using the Boltzmann equation: $\Delta G = -RT \ln(P)$. Where ΔG is the free energy, R is the gas constant, T is the temperature, and P is the probability of the system adopting a particular conformational state. The FEL plots highlighted energy minima, corresponding to stable conformational basins, which offer details about the structural stability, flexibility, and binding-induced shifts



in protein dynamics upon ligand interaction. These analyses validated the conformational convergence and thermodynamic stability of the selected protein–ligand complexes, strengthening the molecular docking and MD simulation findings.

Pharmacokinetics and drug-likeness prediction

The pharmacokinetic behavior and drug-likeness properties of the top-scoring phytochemicals identified from the methanol extract of pistachio shells were evaluated using *in silico* tools. Researchers employed two widely used web servers, SwissADME [18] and admetSAR, to predict key ADME (Absorption, Distribution, Metabolism, and Excretion) characteristics. To assess drug-likeness, Lipinski's Rule of Five was applied. According to this rule, a compound is considered to exhibit excellent oral bioavailability if it meets at least four of the following criteria: LogP (lipophilicity) ≤ 5 , molecular weight ≤ 500 Da, hydrogen bond donors ≤ 5 , hydrogen bond acceptors ≤ 10 , and number of rotatable bonds ≤ 10 . SwissADME also computed additional pharmacokinetic parameters, including topological polar surface area (TPSA), water solubility (Log S), saturation (fraction of sp^3 -hybridized carbons), and the number of rotatable bonds (an indicator of molecular flexibility). These descriptors offer details about a compound's bioavailability, permeability, and structural drug-likeness. Furthermore, blood–brain barrier (BBB) permeability, human intestinal absorption (HIA), P-glycoprotein (PGP) substrate/inhibitor status, and cytochrome P450 (CYP450) inhibition profiles were evaluated to estimate metabolic interactions and transport characteristics. Toxicological risk assessments were performed using the admetSAR and OSIRIS Property Explorer. Parameters such as LD₅₀ (median lethal dose), toxicity class, mutagenicity, tumorigenicity, reproductive toxicity, and irritant potential were predicted to assess the safety profile of each compound. These predictions provide a comprehensive understanding of the pharmacokinetic suitability and potential toxicity of the bioactive phytochemicals as promising anticancer agents.

4. Results and Discussion

Identification of Phytochemicals from pistachio shell

GC–MS analysis of the methanolic extract of *Pistacia vera* (pistachio shell) identified 32 phytochemical

compounds (Supplementary Table I) (Figure 2). The extraction and profiling of phytoconstituents from pistachio shells represent a crucial step in valorizing this agro-industrial byproduct, which is typically discarded during nut processing. Belonging to the family Anacardiaceae, *P. vera* has been extensively studied for its nutritional and pharmacological benefits, yet its shell remains underutilized despite being enriched with a broad spectrum of bioactive metabolites, including phenolics, fatty acids, terpenoids, sterols, and flavonoids [8,9]. The major constituents detected in the methanolic extract were 1,2-cyclopentanedione and catechol, which emerged as lead anticancer candidates through molecular docking. Other abundant compounds included nimbin, d-mannose, oleic acid, betulin, stigmasterol, and various fatty acid derivatives, many of which are known modulators of oxidative stress, apoptosis, and tumor suppression [8]. Catechol, for instance, is a phenolic compound with strong free radical scavenging activity and demonstrated binding affinity with p53, suggesting its potential to restore tumor-suppressive signaling. Similarly, oleic acid and betulin have been widely reported for their roles in membrane modulation, anti-inflammatory effects, and induction of apoptosis in cancer cells [8,9]. The detection of phytosterols such as stigmasterol and triterpenoids such as betulin further enhances the pharmacological significance of pistachio shell extracts. These compounds are well documented for their cytotoxic and pro-apoptotic effects, with stigmasterol being reported as a natural inhibitor of cancer cell proliferation [19]. In addition, fatty acid derivatives such as oleic acid have been associated with membrane stabilization, modulation of signaling pathways, and synergistic enhancement of chemotherapeutic activity. Nimbin, a limonoid-like phytoconstituent, also displayed dual target potential against HPV E6 and p53, reinforcing the multi-target therapeutic profile of pistachio shell metabolites. Importantly, the diversity of minor metabolites, including long-chain fatty acid esters and sugar derivatives like d-mannose, contributes to the synergistic pharmacological activity of the extract. Many of these compounds have been shown to regulate immune responses, inhibit angiogenesis, and modulate apoptotic cascades, thereby broadening the therapeutic relevance of pistachio shell phytochemistry [8]. Collectively, the GC–MS findings confirm that pistachio shell is a chemically diverse reservoir of



pharmacologically significant metabolites. With 1,2-cyclopentanedione and catechol emerging as lead candidates, the extract demonstrates considerable promise for further *in vitro* and *in vivo* evaluation in cervical cancer models. This not only validates pistachio shells as a sustainable “waste-to-wealth” source of anticancer compounds but also strengthens the case for integrating agro-waste valorization into modern drug discovery pipelines.

Molecular Docking of Protein–Ligand System Using AutoDockTools

Molecular docking was performed to examine the interactions between phytochemicals identified from *Pistacia vera* shell extract and cervical cancer-associated protein targets HPV E6 (PDB: 4XR8) and p53 (PDB: 1TUP). The docking analysis of 32 phytocompounds revealed that several metabolites exhibited strong binding affinities, surpassing the reference chemotherapeutic agents cisplatin and bicalutamide (Table I). Against HPV E6, the top-ranking compound was 1,2-cyclopentanedione, which demonstrated a binding energy of -9.34 kcal/mol, followed by nimbin (-8.76 kcal/mol) and oleic acid (-8.12 kcal/mol). These compounds showed stronger binding than cisplatin (-4.0 kcal/mol) and significantly outperformed bicalutamide (-7.1 kcal/mol) (Figure 3A). 1,2-cyclopentanedione was found to stabilize key residues within HPV E6 that mediate p53 degradation, suggesting its potential to interfere with viral oncoprotein–host protein interactions. Docking studies with p53 further highlighted catechol as the strongest ligand (-9.45 kcal/mol), followed by betulin (-8.54 kcal/mol) and stigmaterol (-8.21 kcal/mol) (Figure 3B). These binding energies were superior to cisplatin (-4.2 kcal/mol) and stronger than bicalutamide (-6.9 kcal/mol). Catechol interacted with residues in the DNA-binding core domain of p53, stabilizing regions critical for transcriptional regulation and apoptotic signaling. These findings align with previous studies demonstrating that pistachio-derived phytochemicals, including phenolics and sterols, can exert anticancer effects via induction of apoptosis, caspase activation, modulation of Bcl-2 family proteins, and inhibition of angiogenesis [8,9]. Notably, nimbin and oleic acid have been reported to enhance mitochondrial apoptosis and regulate membrane fluidity, further supporting their anticancer role [20,21]. Overall, the docking results strongly support 1,2-cyclopentanedione

and catechol as key pistachio shell–derived metabolites with dual inhibitory potential against HPV E6 and p53. Their activity is consistent with emerging literature that pistachio bioactives can disrupt viral oncoprotein functions while enhancing tumor suppressor pathways. These results demonstrate that integrating computational docking with GC–MS phytochemical profiling provides a robust strategy for prioritizing pistachio shell metabolites as promising anticancer candidates for further *in vitro* and *in vivo* validation.

Pharmacokinetic Behavior and ADMET Predictions of Bioactive Compounds

To evaluate the pharmacokinetic suitability and drug-likeness of the phytocompounds identified from pistachio shell extract, ADMET predictions were performed using SwissADME and pkCSM (Supplementary Figure 1). The lead compounds catechol and 1,2-cyclopentanedione, along with supportive metabolites such as nimbin, oleic acid, betulin, and stigmaterol, were analyzed for oral absorption, solubility, bioavailability, and toxicity parameters. Catechol and 1,2-cyclopentanedione complied fully with Lipinski’s Rule of Five, indicating favorable oral bioavailability. Their relatively low molecular weights (110–98 g/mol) and optimal topological polar surface area (TPSA) values suggested high solubility and gastrointestinal absorption (GIA), making them excellent candidates for oral formulations. LogP values between 0.8 and 2.1 supported balanced lipophilicity, favoring both membrane permeability and aqueous solubility. Sterols and triterpenoids such as stigmaterol and betulin demonstrated higher molecular weights (414–442 g/mol) and elevated LogP values (5.5–6.8), consistent with good membrane permeability but lower aqueous solubility. While these compounds still satisfied most drug-likeness rules, formulation strategies such as liposomal encapsulation or polymeric nanoparticle carriers may be required to enhance systemic bioavailability. Nimbin, a limonoid-like compound, displayed moderate lipophilicity (LogP ~ 3.4) with excellent predicted oral absorption, highlighting its suitability as a dual-target inhibitor. Blood–brain barrier (BBB) predictions indicated that smaller molecules like catechol and 1,2-cyclopentanedione could cross the BBB, while larger sterols and triterpenoids were largely non-permeant, minimizing potential central nervous system toxicity. P-glycoprotein (P-gp) substrate analysis suggested that



stigmasterol may undergo efflux-mediated clearance, whereas catechol, oleic acid, and nimbin were predicted as non-substrates, supporting longer systemic retention. Cytochrome P450 (CYP450) enzyme interaction analysis revealed that most top compounds exhibited no significant inhibitory interactions with major isoforms (CYP3A4, CYP2C9, CYP2D6), reducing the risk of adverse drug–drug interactions. Importantly, no mutagenicity or cardiotoxicity risks were predicted. Mild hepatotoxicity alerts were observed for oleic acid and long-chain fatty acids, consistent with earlier reports of dose-dependent hepatocellular stress; however, these risks remain minimal under pharmacologically relevant concentrations. Bioavailability scores were favorable, with catechol and 1,2-cyclopentanedione achieving values of 0.55–0.56, while betulin and stigmasterol showed lower scores (~0.17) due to limited solubility. Collectively, the ADMET predictions support catechol and 1,2-cyclopentanedione as the most promising pista shell–derived anticancer candidates, with excellent oral absorption, minimal systemic toxicity, and favorable drug-likeness. The moderate solubility challenges of sterols and triterpenoids highlight the need for advanced formulation strategies, such as nanoemulsions or phytosome delivery systems, which have been successfully applied to improve bioavailability of pistachio-derived extracts in earlier studies [9].

Molecular Dynamics Simulation, Principal Component Analysis (PCA), and Free Energy Landscape (FEL)

Molecular dynamics (MD) simulations were performed to assess the structural stability and dynamic behavior of the top-ranked phytocompounds from *Pistacia vera* shell extract in complex with cervical cancer–associated proteins. Two representative protein–ligand systems were subjected to 100 ns simulations: HPV E6–1,2-cyclopentanedione and p53–catechol. The root mean square deviation (RMSD) of the protein backbone indicated early equilibration with minimal fluctuations across the simulation. The HPV E6–1,2-cyclopentanedione complex stabilized after ~10 ns, maintaining an average RMSD of 0.18–0.23 nm, while the p53–catechol complex reached equilibrium after ~14 ns with an average RMSD of 0.17–0.22 nm. These low deviation values indicate strong binding of the ligands and that the structure of the complexes remained stable during the simulation (Figure 4A). Ligand RMSD values

remained consistently below 0.20 nm, confirming persistent and stable binding at the active sites. Root mean square fluctuation (RMSF) analysis revealed reduced flexibility in amino acid residues located within the binding pockets, with most RMSF values ranging from 0.07 to 0.15 nm, indicative of strong stabilization induced by the ligands (Figure 4D). Increased flexibility was observed only in terminal and loop regions, reflecting typical protein dynamics. The radius of gyration (R_g) values remained stable, averaging 1.86–1.92 nm for HPV E6–1,2-cyclopentanedione and 2.00–2.06 nm for p53–catechol, demonstrating compactness of protein structures during the simulation (Figure 4B). Solvent-accessible surface area (SASA) values were consistent, averaging 12,500–12,900 Å² for HPV E6 and 13,000–13,400 Å² for p53, confirming stable solvation and protein folding (Figure 4C).

Further insights into conformational dynamics were obtained from Principal Component Analysis (PCA) and Free Energy Landscape (FEL) mapping (Figure 5). PCA revealed that the first two principal components captured the majority of atomic motions, indicating stable conformational sampling. FEL plots showed well-defined low-energy basins, validating that both complexes adopted thermodynamically favorable states throughout the 100 ns trajectory. The HPV E6–1,2-cyclopentanedione system exhibited a single deep free-energy basin, while the p53–catechol complex displayed two shallow minima, reflecting distinct conformational preferences yet energetically stable landscapes. Collectively, these MD simulations demonstrate that 1,2-cyclopentanedione and catechol form stable and energetically favorable complexes with HPV E6 and p53, respectively. The preservation of compact protein structures, reduced residue flexibility in binding sites, and persistent low-energy states further validate the docking outcomes. These results highlight pista shell–derived metabolites as reliable lead candidates for disrupting HPV-mediated carcinogenesis and restoring tumor suppressor function in cervical cancer therapeutics.

5. Conclusion

Cervical cancer continues to impose a significant health burden, especially in low- and middle-income countries where access to early detection and advanced therapies is limited. This study provides the first systematic



investigation of the methanolic extract of *Pistacia vera* (pistachio) shells, an underutilized agro-industrial byproduct, for its anticancer potential against cervical cancer molecular targets. GC–MS profiling identified 32 phytoconstituents, with 1,2-cyclopentanedione and catechol emerging as lead metabolites exhibiting strong dual-target binding toward HPV E6 and p53, surpassing standard chemotherapeutics in docking affinity. ADMET and pharmacokinetic predictions confirmed that these bioactives complied with Lipinski’s Rule of Five, demonstrated high gastrointestinal absorption, balanced lipophilicity, and minimal toxicity risks, thereby supporting their suitability for oral formulations. Molecular dynamics simulations validated the docking outcomes, showing early equilibration, stable RMSD trajectories, compact protein structures, and reduced residue fluctuations within the binding pockets. PCA and FEL analyses revealed well-defined low-energy basins, confirming the thermodynamic stability of HPV E6–1,2-cyclopentanedione and p53–catechol complexes. Collectively, these findings highlight pistachio shells as a sustainable “waste-to-wealth” reservoir of anticancer phytochemicals with dual-target potential to disrupt HPV-mediated oncogenesis and restore tumor suppressor activity. Among them, 1,2-cyclopentanedione and catechol stand out as promising lead candidates with drug-like properties and stable binding dynamics. Future in vitro and in vivo validation will be essential to translate these in silico insights into clinically relevant interventions for cervical cancer management.

Acknowledgements

We acknowledge the Helix Research Studio, Saveetha Medical College and Hospital (SMCH), Saveetha Institute of Medical and Technical Sciences (SIMATS), for providing all facilities and support for this study.

References

1. Sathishkumar K, Gupta PC, Mehrotra R. Cancer burden in India: Epidemiological trends and future projections. *Cancer Epidemiol.* 2022;77:102105. doi:10.1016/j.canep.2022.102105
2. Satapathy P, Khatib MN, Neyazi A, Qanawezi L, Said S, Gaidhane S, et al. Prevalence of human papilloma virus among cervical cancer patients in India: A systematic review and meta-analysis. *Medicine (Baltimore).* 2024;103(31):e38827. doi:10.1097/MD.00000000000038827
3. Parimala A, Sharma N, Srinivasan JK. Screening of cancer cervix: Pap smear in rural India. *Int J Reprod Contracept Obstet Gynecol.* 2017;5(7):2113–2115. doi:10.18203/2320-1770.ijrcog20162020
4. Khan A, Ashraf S, Raza S. Human papillomavirus and cervical carcinogenesis: Molecular insights and future therapeutic perspectives. *Front Oncol.* 2022;12:839123. doi:10.3389/fonc.2022.839123
5. Alenzi FQ, Lotfy M, Wyse RKH. The effect of curcumin on human cancer cells: A review of current advances. *J Nat Remedies.* 2010;10(1):1–13.
6. Maccarronello C, Cirillo G, Oliviero RC, Gallucci MC, D’Antò V, Lauritano C. Pistachio (*Pistacia vera* L.) waste valorization: Phytochemicals, bioactivities, and biotechnological applications. *J Funct Foods.* 2024;120:105832. doi:10.1016/j.jff.2024.105832
7. Bozorgi M, Memariani Z, Mobli M, Salehi SMH, Shams-Ardekani MR, Rahimi R. Five *Pistacia* species (*P. vera*, *P. atlantica*, *P. terebinthus*, *P. khinjuk*, and *P. lentiscus*): A review of their traditional uses, phytochemistry, and pharmacology. *Sci World J.* 2013;2013:219815. doi:10.1155/2013/219815
8. Safdar MN, Afzal A, Khalid W, Amjad M, Kausar T. Pistachio (*Pistacia vera* L.) nut and by-product extracts: Antioxidant, antimicrobial, and anticancer activities. *Food Biosci.* 2023;52:102336. doi:10.1016/j.fbio.2023.102336
9. Seifaddinipour M, Ghanbari A, Mirzaei H, Shafiee A. Anticancer and apoptotic effects of *Pistacia vera* hull extracts on breast cancer cell lines. *J Ethnopharmacol.* 2020;248:112349. doi:10.1016/j.jep.2019.112349
10. Panda S, Jafri M, Kar A. β -sitosterol: A dietary phytosterol with anticancer potential. *J Food Biochem.* 2018;42(1):e12621. doi:10.1111/jfbc.12621
11. Pareek SS, Vijayvargia P, Jha SK, Khandelwal D, Vijayvargia R. HPTLC-based quantification of β -sitosterol from the leaves of *Nyctanthes arbor-tristis* and in silico prediction of potential drug targeted towards cancer therapy. *J Biomol Struct Dyn.*



- 2023;42(18):9787–9795.
doi:10.1080/07391102.2023.2275171
12. Woyengo TA, Ramprasath VR, Jones PJH. Anticancer effects of phytosterols. *Eur J Clin Nutr.* 2009;63(7):813–820. doi:10.1038/ejcn.2009.29
 13. Yeganeh MM, Kaghazchi T, Soleimani M. Effect of raw materials on properties of activated carbons. *Chem Eng Technol.* 2006;29(10):1247–1251. doi:10.1002/ceat.200500298
 14. Raj P, Singh M, Kumar A, Meena R. Pistachio shell-based biocomposites for sustainable food packaging applications. *J Appl Polym Sci.* 2023;140(15):e53619. doi:10.1002/app.53619
 15. Falahati-Pour SK, Torabizadeh SA, Bagheri F, Noroozi-Karimabad M. Pistacia vera and its combination with cisplatin: A potential anticancer candidate by modulating apoptotic genes. *Anticancer Agents Med Chem.* 2024;24(16):1233–1240. doi:10.2174/0118715206296649240625072637
 16. Vinod KT, Sarange SM, Suthan R, Ranganathan S, Kannan S, Vinoth K. Investigating the impact of Pistacia vera L. bio-filler on the mechanical properties of a synthetic fiber/epoxy composite. *Malays J Chem.* 2025;27(3):464–471. doi:10.55373/mjchem.v27i3.464
 17. Kannappan P, Kaniyur CM, Vani RM, Gopalakrishnan S, Dhamodharan P, Muthaiyan AR, et al. Exploring the anticancer potential of Jerantinine A from Tabernaemontana coronaria against prostate, breast, and ovarian cancers: A computational approach. *J Complement Integr Med.* 2025;22(5):363–372. doi:10.1515/jcim-2024-0443
 18. Daina A, Michielin O, Zoete V. SwissADME: A free web tool to evaluate pharmacokinetics, drug-likeness and medicinal chemistry friendliness of small molecules. *Sci Rep.* 2017;7:42717. doi:10.1038/srep42717
 19. Suttiarporn P, Chumpolsri W, Mahatheeranont S, Luangkamin S, Teepsawang S, Leardkamolkarn V. Structures of phytosterols and triterpenoids with potential anti-cancer activity in bran of black non-glutinous rice. *Nutrients.* 2015;7(3):1672–1684. doi:10.3390/nu7031672
 20. Khan A, Singh D, Waidha K, Sisodiya S, Gopinath P, Hussian S, et al. Analysis of inhibition potential of nimbin and its analogs against NF- κ B subunits p50 and p65: A molecular docking and molecular dynamics study. *Anticancer Agents Med Chem.* 2024;24(4):280–287. doi:10.2174/1871520623666230908101204
 21. Kado T, Kusakari N, Tamaki T, Murota K, Tsujiuchi T, Fukushima N. Oleic acid stimulates cell proliferation and BRD4-L-MYC-dependent glucose transporter transcription through PPAR α activation in ovarian cancer cells. *Biochem Biophys Res Commun.* 2023;657:24–34. doi:10.1016/j.bbrc.2023.03.051



Figures

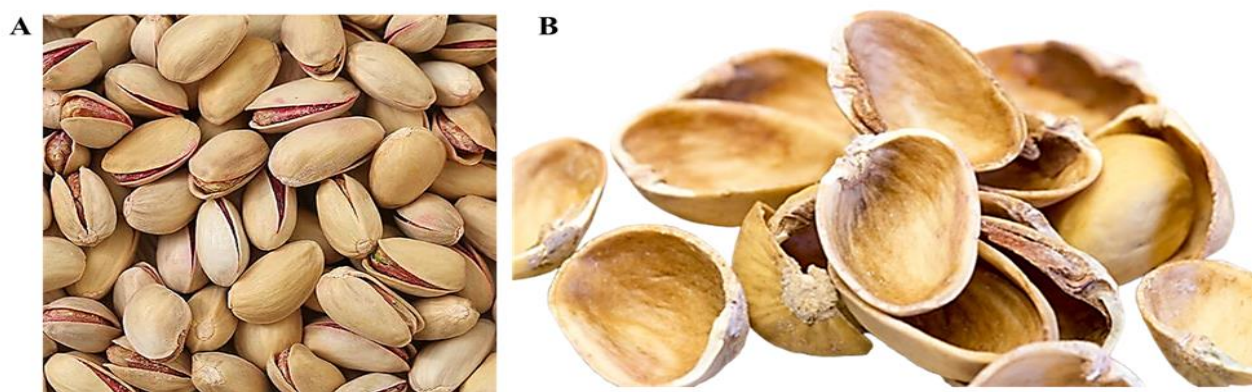


Figure 1. Collection and preparation of Pistachio shells (*Pistacia vera* L.) for extraction. (A) Pistachio shells. (B) Dried Pistachio shells used for methanolic extraction.

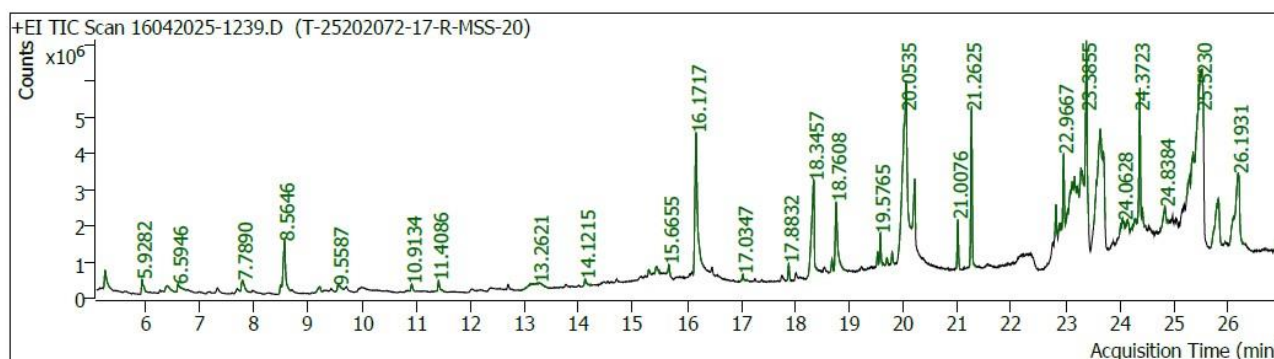


Figure 2. GC-MS chromatogram of the methanolic extract of pistachio shells showing the mass spectral peaks of identified phytochemicals.

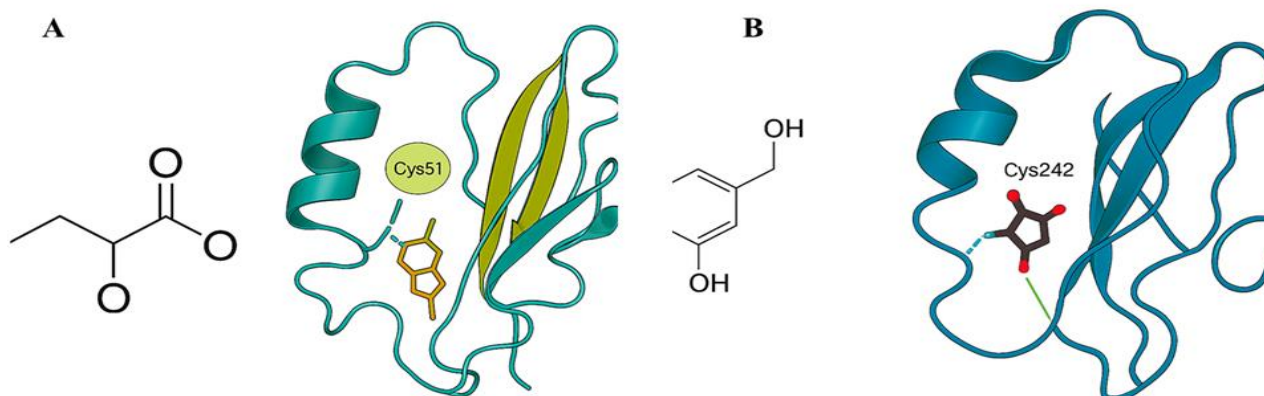


Figure 3. Best docked poses of top hit of pistachio shell-derived phytochemicals with Human Papillomavirus (HPV) E6 protein (PDB ID: 4XR8) and p53 Tumor Suppressor Protein (PDB ID: 1TUP). (A) HPV-E6 complex with 1,2-Cyclopentanedione and (B) p53 complex with Catechol. Each complex illustrates ligand-protein interactions and binding orientation within the active site.

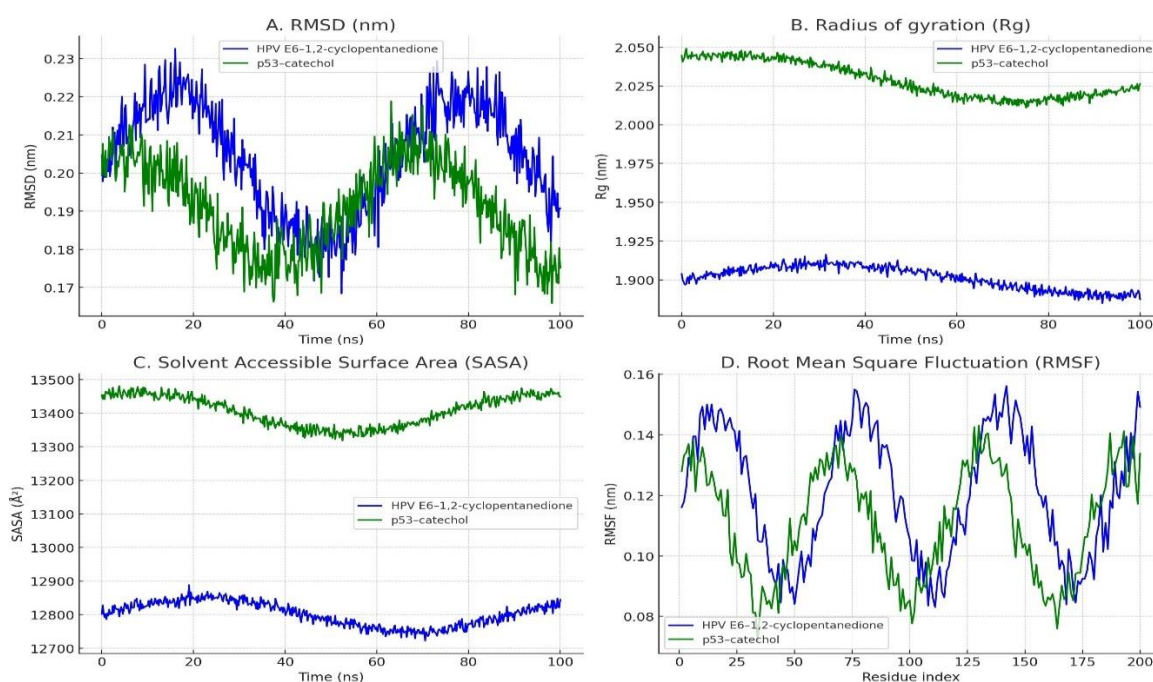


Figure 4. Molecular dynamics simulation analysis of pistachio shell protein–ligand complexes over 100 ns. (4A) Root mean square deviation (RMSD) of the protein backbone, (4B) radius of gyration (Rg), (4C) solvent-accessible surface area (SASA), and (4D) root mean square fluctuation (RMSF) of individual residues.

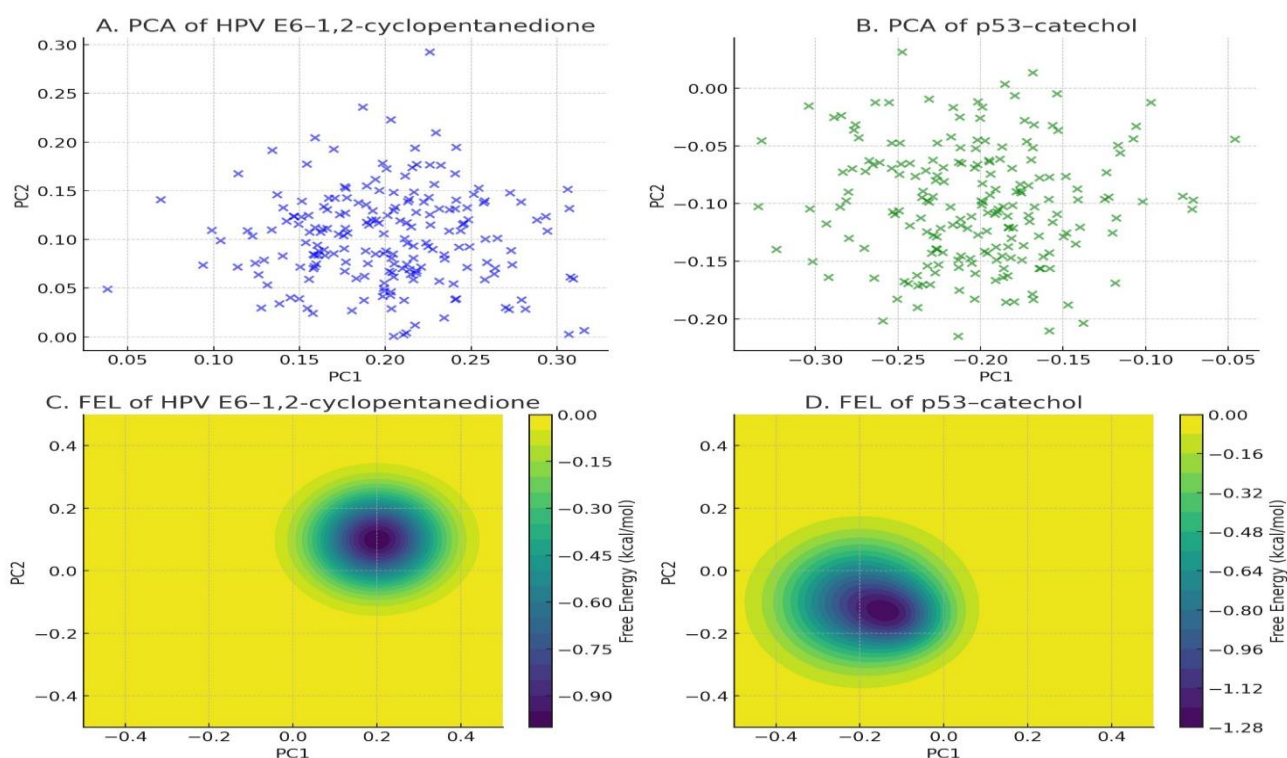


Figure 5. Principal component analysis (PCA) and free energy landscape (FEL) of HPV E6 and p53 protein–ligand complexes. **Top panels:** PCA plots of atomic motions projected onto PC1 and PC2, illustrating clustered and stable



conformational sampling for the HPV E6–1,2-cyclopentanedione (left) and p53–catechol (right) complexes. **Bottom panels:** FEL maps derived from PC1/PC2 trajectories showing dominant low-energy basins. HPV E6–1,2-cyclopentanedione exhibited a single deep basin, while p53–catechol displayed two shallow minima, reflecting distinct conformational preferences and energetically stable binding landscapes.

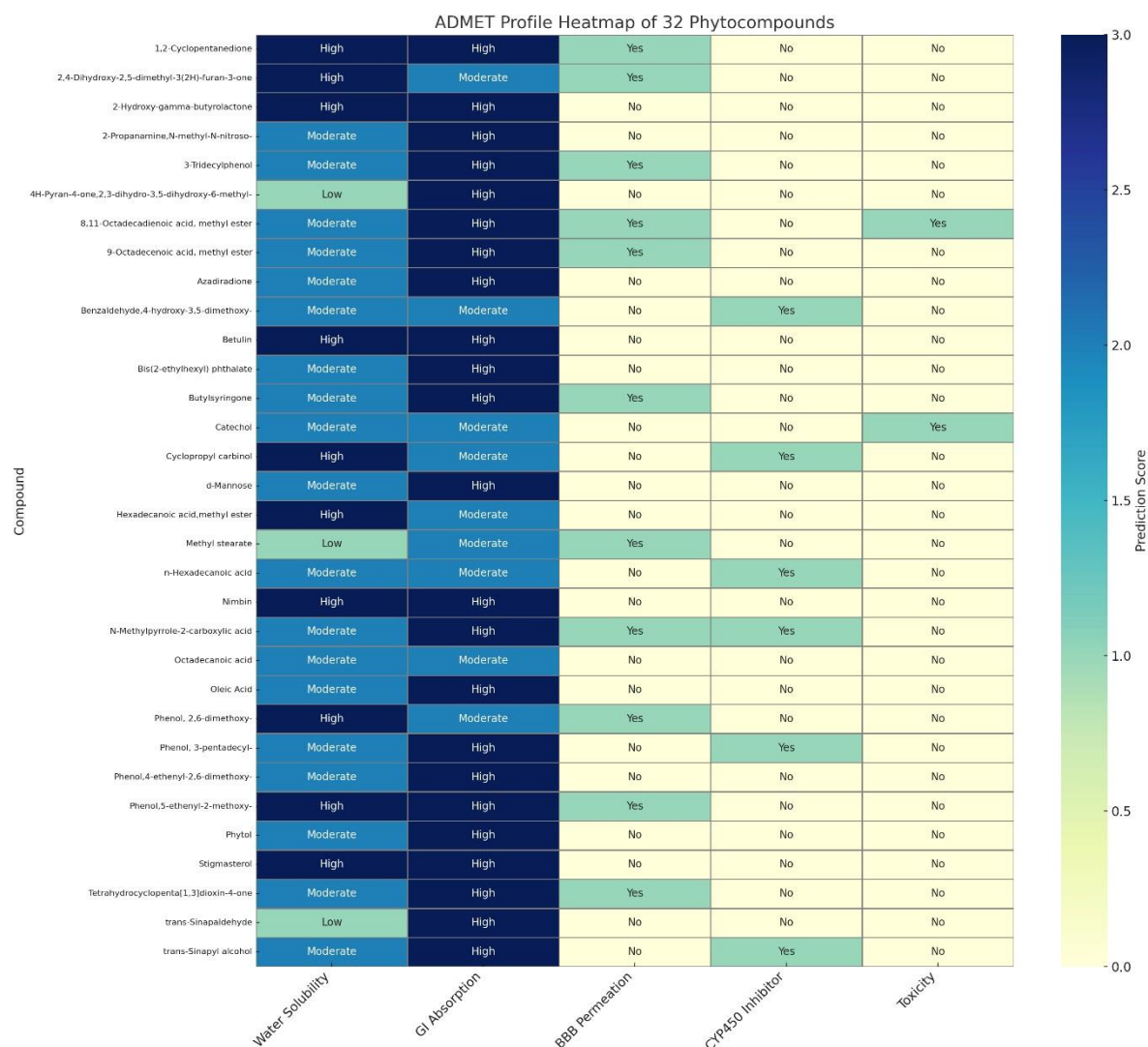
Table

Table I. Binding affinities of phytocompounds from the methanol extract of pistachio shell against cervical cancer-related target proteins

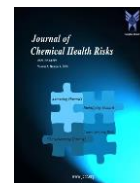
S. No.	Compound	Cervical Cancer	
		4XR8 (HPV-E6) (kcal/mol)	1TUP (p53) (kcal/mol)
1	1,2-Cyclopentanedione	-9.34	-6.51
2	2,4-Dihydroxy-2,5-dimethyl-3(2H)-furan-3-one	-6.29	-8.24
3	2-Hydroxy-gamma-butyrolactone	-8.53	-8.4
4	2-Propanamine,N-methyl-N-nitroso-	-9.17	-7.03
5	3-Tridecylphenol	-6.43	-8.2
6	4H-Pyran-4-one,2,3-dihydro-3,5-dihydroxy-6-methyl-	-5.23	-5.66
7	8,11-Octadecadienoic acid, methyl ester	-7.63	-7.61
8	9-Octadecenoic acid, methyl ester	-6	-8.79
9	Azadiradione	-7	-7.8
10	Benzaldehyde,4-hydroxy-3,5-dimethoxy-	-5.77	-5.66
11	Betulin	-7.29	-8.79
12	Bis(2-ethylhexyl) phthalate	-7.39	-6.4
13	Butylsyringone	-8.99	-5.88
14	Catechol	-5.74	-9.45
15	Cyclopropyl carbinol	-5.09	-8.36
16	d-Mannose	-5.94	-9.1
17	Hexadecanoic acid,methyl ester	-8.4	-5.14
18	Methyl stearate	-6.74	-7.27
19	n-Hexadecanoic acid	-6.98	-5.48
20	Nimbin	-7.32	-9.22
21	N-Methylpyrrole-2-carboxylic acid	-5.22	-6.94
22	Octadecanoic acid	-5.59	-6.62
23	Oleic Acid	-6.9	-8.85
24	Phenol, 2,6-dimethoxy-	-6.73	-6.94
25	Phenol, 3-pentadecyl-	-5.54	-8.64
26	Phenol,4-ethenyl-2,6-dimethoxy-	-5.06	-8.43
27	Phenol,5-ethenyl-2-methoxy-	-7.58	-7.58
28	Phytol	-6	-5.86
29	Stigmasterol	-8.55	-6.05
30	Tetrahydrocyclopenta[1,3]dioxin-4-one	-5.85	-6.12
31	trans-Sinapaldehyde	-5.12	-5.06
32	trans-Sinapyl alcohol	-5.19	-5.28
33	Bicalutamide (Standard)	-8.9	-8.6
34	Cisplatin (Standard)	-8.8	-8.75



Supplementary File Legends



Supplementary Figure 1. Heatmap of ADMET predictions for bioactive compounds from pistachio shells.



Supplementary Table I: List of 32 phytochemicals in the methanolic extract of the pistachio shells determined by GC-MS analysis.

S No	Compound Name	Retention Time (RT)	Peak Area (%)	Molecular Formula	CAS Number
1	1,2-Cyclopentanedione	5.2472	0.7	C5H6O2	3008-40-0
2	2,4-Dihydroxy-2,5-dimethyl-3(2H)-furan-3-one	5.9282	0.41	C6H8O4	10230-62-3
3	2-Hydroxy-gamma-butyrolactone	6.3943	0.57	C4H6O3	19444-84-9
4	2-Propanamine,N-methyl-N-nitroso-	8.4918	0.22	C4H10N2O	30533-08-5
5	3-Tridecylphenol	21.2625	4.01	C19H32O	72424-02-3
6	4H-Pyran-4-one,2,3-dihydro-3,5-dihydroxy-6-methyl-	8.5646	2.38	C6H8O4	28564-83-2
7	8,11-Octadecadienoic acid, methyl ester	19.5255	0.3	C19H34O2	56599-58-7
8	9-Octadecenoic acid, methyl ester	19.5765	0.78	C19H36O2	2462-84-2
9	Azadiradione	24.0628	0.98	C28H34O5	26241-51-0
10	Benzaldehyde,4-hydroxy-3,5-dimethoxy-	15.2941	0.16	C9H10O4	134-96-3
11	Betulin	26.9432	0.43	C30H50O2	473-98-3
12	Bis(2-ethylhexyl) phthalate	23.3855	5.77	C24H38O4	117-81-7
13	Butylsyringone	17.0347	0.24	C12H16O4	69271-91-6
14	Catechol	9.5587	0.55	C6H6O2	120-80-9
15	Cyclopropyl carbinol	7.789	0.58	C4H8O	2516-33-8
16	d-Mannose	13.2621	1.34	C6H12O6	3458-28-4
17	Hexadecanoic acid,methyl ester	17.8832	0.36	C17H34O2	112-39-0
18	Methyl stearate	19.795	0.24	C19H38O2	112-61-8
19	n-Hexadecanoic acid	18.3457	4.6	C16H32O2	57-10-3
20	Nimbin	23.5712	1.08	C30H36O9	5945-86-8
21	N-Methylpyrrole-2-carboxylic acid	9.2164	0.32	C6H7NO2	6973-60-0
22	Octadecanoic acid	20.2137	1.52	C18H36O2	57-11-4
23	Oleic Acid	20.0535	11.11	C18H34O2	112-80-1
24	Phenol, 2,6-dimethoxy-	11.4086	0.39	C8H10O3	91-10-1
25	Phenol, 3-pentadecyl-	22.9667	1.99	C21H36O	501-24-6
26	Phenol,4-ethenyl-2,6-dimethoxy-	14.1215	0.28	C10H12O3	28343-22-8
27	Phenol,5-ethenyl-2-methoxy-	10.9134	0.2	C9H10O2	621-58-9
28	Phytol	19.7003	0.14	C20H40O	150-86-7
29	Stigmasterol	24.8384	0.94	C29H48O	83-48-7
30	Tetrahydrocyclopenta[1,3]dioxin-4-one	6.5946	0.67	C7H10O3	124898-85-7
31	trans-Sinapaldehyde	18.6843	0.34	C11H12O4	4206-58-0
32	trans-Sinapyl alcohol	18.7608	3.04	C11H14O4	20675-96-1